

Chemical Releases at High Altitudes

Controlled release of chemicals from research rockets leads to new knowledge about the upper atmosphere.

N. W. Rosenberg

Man's attempts at controlled modification of the earth's lower atmosphere are frustrated by the sheer mass, on a geophysical scale, of the air itself. At sea level, a single cubic kilometer contains a million tons of air. In terms of "chemical release" the daily exhaust products of all the motor vehicles of the world, if collected, would barely fill this volume at normal pressures. However, atmospheric pressure decreases so rapidly with height that at an altitude of 150 kilometers, the mass of air in a cubic kilometer totals less than 2 kilograms (1). This mass can be completely displaced by the release of the contents of a gas cylinder easily carried to this height by a small research rocket.

Such "artificial modification" can produce effects which may be recorded by simple ground-based instruments and which can tell us much about the region in which they occur. It is emphasized that experiments of this type do not have as an objective the modification of weather in the earth's lower atmosphere and are inherently limited to the role of a research tool in increasing our knowledge about the upper atmosphere. Within that framework, they have been highly successful in the measurement of

winds, diffusion, and temperature at altitudes between 80 and 200 kilometers. They have also been useful in studying chemical composition and reaction rates, the characteristics of radio-wave reflections from layers of ionized constituents, and dissipation of sound-wave energy in this region. In some of these studies, they provide unique measurements of properties not readily determined by other methods; in other studies, they provide cross-checks of experimental measurements made by other methods.

It had long been recognized that a major source of light in the twilight sky is a thin layer of free sodium atoms centered at a height of 90 kilometers, which absorbs and reemits sunlight at the sodium resonance wavelength of 5890 angstroms. Since the layer contains only a fraction of a kilogram of sodium per square kilometer across its entire thickness, it was suggested in 1950 by Bates (2) that injection of as little as 1 kilogram of sodium vapor from a rocket could visibly increase emission over an area of several square kilometers. The first experiment, made by Edwards, Bedinger, Manning, and Cooper from White Sands, New Mexico, in 1955 (3), was the twilight release of 3 kilograms of sodium vapor between 70 and 113 kilometers altitude from an Aerobee rocket. This release

created a brilliant yellow trail (5890 Å resonance) above 85 kilometers, soon distorted by ionospheric winds, and growing to over 1 kilometer in diameter, disappearing only as sunset at altitude left it in darkness.

The simplicity of the experiment for wind measurements has led to its widespread use as a first step in rocket research by various nations. Cooperative coordinated launches have been organized within the framework of the Committee on Space Research (COSPAR), and between 1958 and 1965 about 100 wind profiles have been obtained and analyzed by groups in the United States, France, Canada, Italy, Great Britain, Japan, Argentina, India, and Pakistan (4).

The use of the same sodium trails to estimate diffusion rates and temperatures has also been successful. Measurement of the rate of growth of the trail width provides one of the few experimental methods to test theoretically predicted upper-atmosphere diffusion rates (5). Unique determinations of temperature profiles between 100 and 200 kilometers have been made by Blamont (6) through measurement of the Doppler broadening of the resonance emission. Many other release experiments have also been carried out with other chemicals which produce light emissions or local changes in the natural electron density of the ionosphere. This article will survey qualitatively the objectives, methods, and results associated with the use of this general technique in upper-atmosphere research.

Geophysics of Chemical Release

Altitudes at which the chemical release technique has been most useful extend from about 80 to 200 km. The temperature of this region increases from 180°K at 80 km to about 1200°K at 200 km, while density falls from 10^{-5} to 10^{-10} of sea-level density over the same interval. At 80 km, atmospheric composition is very similar to that at the earth's surface, but

The author is a branch chief at the U.S. Air Force Cambridge Research Laboratories, Bedford, Massachusetts.

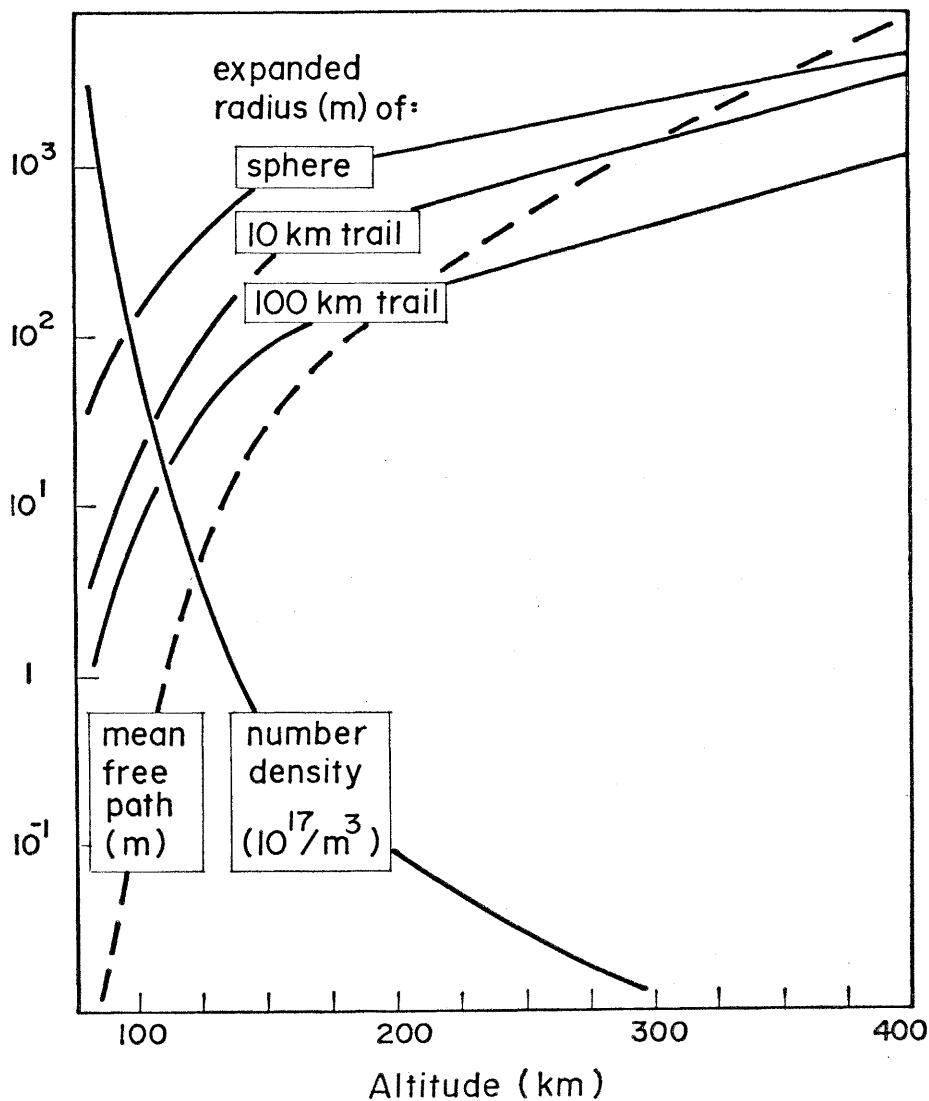


Fig. 1. Atmospheric number density and mean free path plotted against altitude. Calculated radii following pressure equilibration are also shown for release of 10^{26} molecules of gas at a point along a 10-kilometer trail and along a 100-kilometer trail.

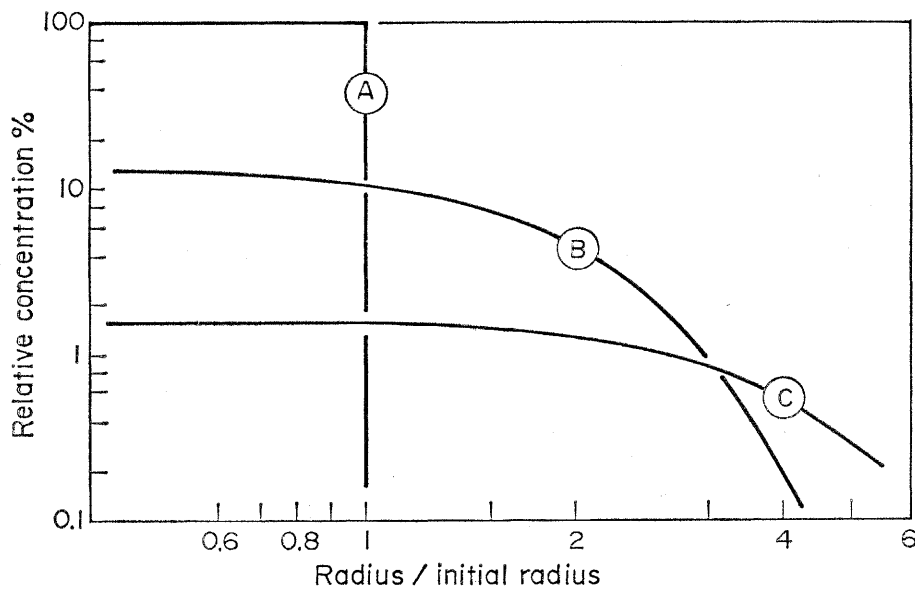


Fig. 2. Spherical diffusional growth of a released gas. Profiles of a relative concentration plotted against radius are shown at three times (A, B, and C) after point release. Circles labeled A, B, and C are located at the effective radius r_e where the relative concentration is $1/e$ centerpoint concentration. The three curves correspond to times of 1, 50, and 250 seconds, respectively, after release of 10^{26} molecules at 120 kilometers.

dissociation of molecular oxygen into atomic oxygen becomes significant at 90 km, amounts to 50 percent at 110 km, and is over 90 percent at 200 km. Ionized gases, although they form only a very small fraction of total gases, are important in radio propagation. They provide daytime electron (and positive ion) densities ranging from 10^3 electrons per cubic centimeter at 80 km to 10^5 at 100 km and to 10^6 at 200 km.

The total number density (of molecules and atoms) and the mean free path between collisions are two properties of the upper atmosphere which most directly control the expansion and mixing of released chemicals. Their average values, shown in Fig. 1, as well as most other values given in this article, are significant to only one or two figures because of geophysical variabilities.

The net weight of chemical is limited to a few kilograms by the cost of larger rockets, but the chemical can be released either at a single point to form a spherical injection zone, or continuously as a long trail along the rocket trajectory to form a cylindrical injection zone. An estimate of the space occupied by the released gas following injection can be made by assuming that the gas first expands radially, forming a "bubble" without intermixing until its pressure falls to that of the surrounding air. (This is an oversimplification of the initial expansion, which includes energy expenditure to form shock waves.) If the payload temperature is selected so as to provide an expanded bubble temperature equal to ambient temperature, equal pressure is obtained when the number density of the released gas is equal to the number density n_a in the ambient atmosphere. This condition is met in the point release when $n_a = N_0/4\pi r_1^3/3$ and in the trail release when $n_a = N_0/\pi r_1^2 L$ where N_0 is the total number of released molecules, r_1 the bubble radius following pressure equilibration, and L the trail length. Release of 10^{26} atoms or molecules (equivalent to 4 kg Na vapor) leads to values of the bubble radius which range from meters to kilometers, depending on height. They are shown in Fig. 1 for spherical "point" releases and for cylindrical trails 10 km and 100 km long. The initial expansion to ambient pressure requires a fraction of a second, a time on the order of that required for a molecule at thermal velocity to travel a distance equal to the bubble radius.

After pressure equilibration, diffusion processes control the mixing of the released gas with surrounding air and its eventual dissipation. Molecular diffusion is the dominant process for neutral species above 110 km, and the released chemical develops a Gaussian distribution as this mixing proceeds, governed by the equation

$$n(r,t)/n(0,0) = b^m \exp - (br/r_1)^2$$

where $n(r,t)$ is the number density of the released gas at radius r and time t ; $1/b^2 \equiv 1 + 4Dt/r_1^2$; $m = 2$ for a cylinder, $= .3$ for a sphere; and D is the rate constant for molecular diffusion. From this equation we may extract two simple measures of the extent of diffusion at any given time: (i) the relative centerpoint concentration of released gas $\equiv n(0,t)/n(0,0) = b^m$ and (ii) the effective radius (that is, the radius at which the concentration of the released gas falls to $1/e$ of its centerpoint concentration) $\equiv r_e = r_1 b^{-1}$.

As an example, the point release of 10^{26} molecules at an altitude of 120 km forms a pressure-equilibrated bubble of radius $r_1 = 350$ meters in about 1 second. The released chemical then diffuses outward and surrounding air diffuses inward at such a rate that over 50 seconds, the effective radius doubles to 700 m while the relative centerpoint concentration falls to 12 percent. About 250 seconds are required to quadruple the effective radius to 1400 m, while the relative centerpoint concentration falls to 1.6 percent. This diffusional growth is shown in Fig. 2.

At lower altitudes, molecular diffusion becomes much slower. For example, the time required to double the radius of the 10^{26} -molecule release, which is 50 seconds at an altitude of 120 km, should triple to 150 seconds on moving down to 100 km and triple again to 450 seconds at 80 km. However, at altitudes below 105 km the released gases develop a distinct globular eddy structure within a few seconds after release. These eddies grow rapidly and linearly with time, both in radius and in separation. When a diffusion constant is calculated from the observed growth, its value is at least tenfold higher than that expected for molecular diffusion (5), and it is evident that there is another dominant mixing process. A sharp boundary exists between this apparently turbulent region and the clearly nonturbulent region above it, seen in Figs. 3 and 4. The transition altitude is experimentally

found to be fixed within a few kilometers of 100 km at all times and at all sites from which observations have been made. The altitude is about 5 km lower at sunset than at sunrise. The existence of this boundary has explained the absence of separation among natural atmospheric constituents below 100 km, with the presence of diffusive separation among lighter and heavier species only above this height, where the mo-

lecular diffusion process is the controlling factor.

At higher altitudes, the mean free path increases more rapidly than the bubble radius (compare Fig. 1). At heights where the mean free path is no longer small compared to the bubble radius, the above model, which considers the medium as a continuum rather than as separate molecules, breaks down because the radial velocity

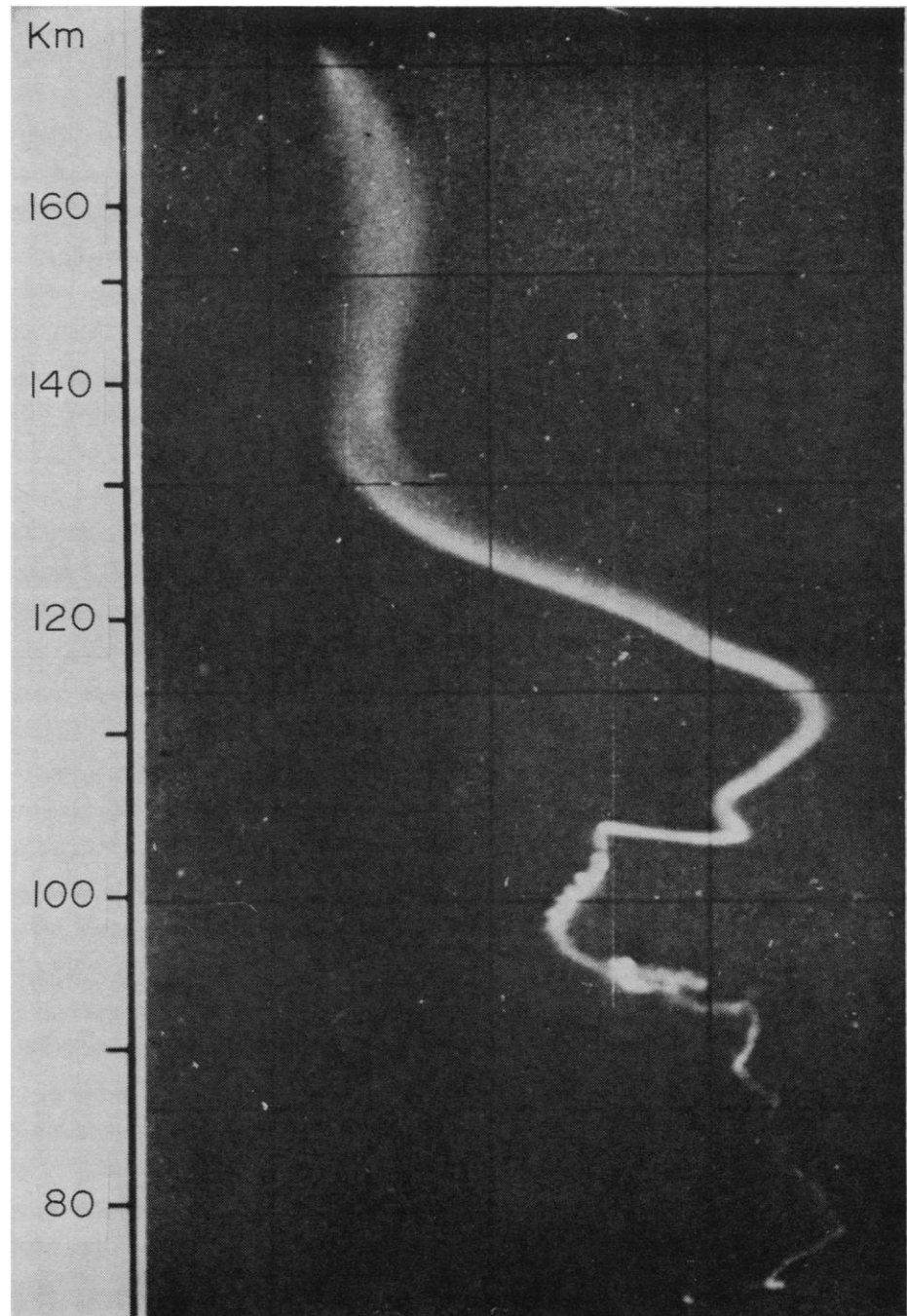


Fig. 3. Sodium trail at twilight, made by release of 2 kilograms of sodium vapor between 60 and 180 kilometers altitude. At time of photograph, the vehicle was still releasing vaporized sodium. Although not evident in a black-and-white photograph, the trail was white (sodium oxide smoke) below 90 kilometers and yellow (sodium atom vapor) above 90 kilometers. Note sharp boundary between turbulent and laminar growth at 104 kilometers. [Photograph provided by H. D. Edwards, Georgia Institute of Technology]

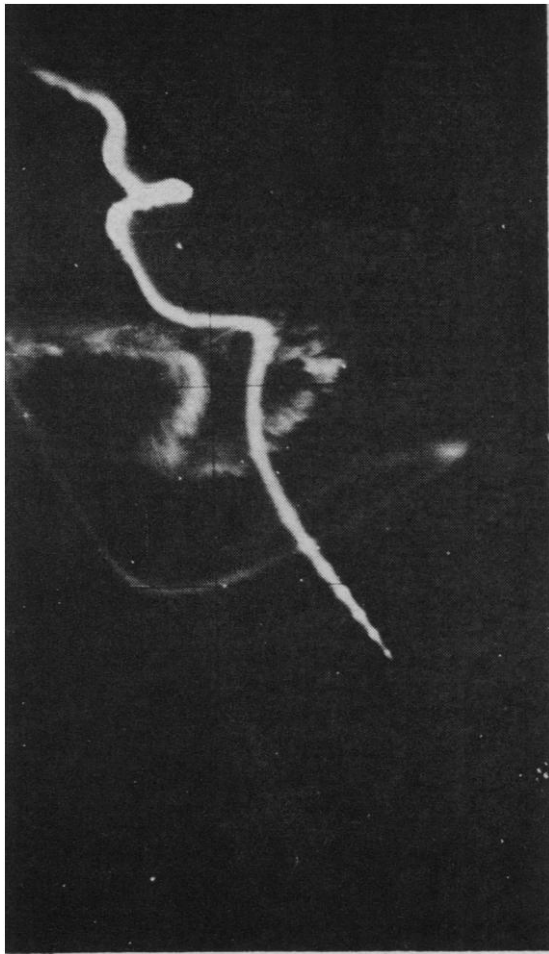


Fig. 4. Two chemiluminous trails, each made by release of 4 kilograms of trimethylaluminum along separate rocket trajectories between 80 and 160 kilometers. Dimmer trail was released 2 minutes before photograph. Second rocket is still releasing trimethylaluminum at 150 kilometers at time of photograph. Puffs were made to estimate vertical speeds. Lower ends of trails are at 87 kilometers altitude; boundary between turbulent and laminar portions is at 105 kilometers. The photograph (provided by H. D. Edwards) was taken from a point 100 kilometers east of the release area, and covers a 30-degree field of view.

of the released gas is not fully randomized, during its expansion to this calculated radius, by collisions with ambient air molecules. Furthermore, at altitudes above 250 km the released gas molecules may travel many kilometers and reach an unusably low concentration before each encounters sufficient collisions to bring it to the velocity and temperature of its surroundings. Observations of ambient winds and temperatures are meaningless until these collisions have occurred, and there is consequently an upper height limit to useful observations. The expansion dynamics in interplanetary space (150,000 km from earth) was studied by a sodium release from a Soviet space probe (see 7).

Release Techniques

Most payloads are carried to the release altitudes in the cylindrical section of a research rocket, which has usually burned out at a much lower altitude. The vehicle is therefore moving along a ballistic trajectory at a typical velocity of 1 km/sec at the time of release. The gas or liquid is released through an orifice selected to give the desired rate of injection, following initiation of the release by a timer. In the case of a pyrotechnic mixture (such as is used to produce the sodium vapor), a small cartridge is fired to ignite it.

One problem in the interpretation of results is that the released chemical is not initially at rest with respect to the atmosphere. Even the controlled injection of a gas through an orifice takes place into a near-vacuum, forming a supersonic jet. Furthermore, the orifice is itself moving supersonically through the atmosphere. These motions create an outer shock wave in the surrounding air and an inner shock in the released gas. Mixing and chemical reactions are confined, at early times, to the space between the two shock surfaces, the radii of which are controlled by the release rate, vehicle velocity, and atmospheric pressure. In a study of the release of nitric oxide into the upper atmosphere (8) this aerodynamic structure was measured, and good agreement between aerodynamically predicted and photographically observed radii was found. It is more difficult to analyze the structure of liquid or particulate releases, for reasons which will be discussed later.

I shall review releases in four categories: those which glow when sunlit, those which glow without sunlight, those which change ambient electron density, and those which result in shock waves. Although a single release may have several of these effects, I shall group it by the principal effect under investigation.

Releases Glowing in Sunlight

In some "tracer" studies, the resonance radiation (in sunlight) of a small quantity of released vapor is observed. The vapor takes on the mass motions and the temperature of the region into which it is injected. In order to measure wind and diffusion profiles with height, the release is recorded by

ground-based narrow-filter cameras over a period of several minutes for triangulation of trail motions. For temperature studies, a ground-based high-resolution photometer or interferometer is used to measure spectral profiles. The release is usually made about 40 minutes after ground sunset (or before ground sunrise) to have the darkest possible sky background while the release is sunlit by solar rays which have not been seriously attenuated.

The sodium release as presently used (9) consists of about 2 kg of sodium powder dispersed in 8 kg of a thermite mixture ($\text{Fe}_2\text{O}_3\text{-Al}$) carefully packed to burn for 200 seconds, ejecting vaporized (900°C) sodium at a rate of about 10 grams per kilometer along the trajectory. At heights above 85 km, the sodium is oxidized only slowly in the ambient air since efficient oxidation requires three-body collisions, which are rare at these densities. The sodium vapor expands to form a trail (such as that of Fig. 3) which takes on ambient wind motions and temperatures.

The wind measurements at 90 to 150 km show very high horizontal speeds (up to 600 km/hr) which change direction rapidly with height, frequently reversing over a height span of a few kilometers, as shown in Fig. 5. Possible sources of both the high speeds and high shears have been examined by several investigators, notably Hines (10). Certain persistent characteristics suggest that several energy sources are operating simultaneously, including diurnal and semidiurnal solar-heating tides, and gravity waves of much shorter periods. The viscous drag (that is, frictional heating) between successive layers moving in different directions even at altitudes where no turbulent structure is present) represents a major source of energy transfer from organized wind motions directly into thermal energy content, that is, increased temperature. This source of heat input can significantly affect the temperature profile at altitudes between 120 and 160 km (10).

For temperature measurements, potassium is preferred to sodium because the earth's natural sodium layer distorts the incoming solar spectrum and makes interpretation difficult. The results of the temperature-profile studies by Blamont (6) are compatible at low heights with temperature measurements by grenade and falling-sphere techniques, and

at higher altitudes with profiles deduced from satellite drag measurements. In the intermediate altitude interval of 110 to 200 km, agreement with theoretical estimates of profiles of temperature as a function of height is reasonably good.

A recent important modification of the metal-vapor release is the development by Föppl and co-workers (11) of a barium-vapor generator in which a small fraction of the released barium is ionized. Neutral barium takes on ambient wind speeds and diffuses spherically, but the Ba^+ ion-electron plasma is confined to diffuse along magnetic field lines at high altitudes. Since the neutral barium resonance emission occurs at a wavelength of 5535 Å and that of ionized Ba^+ at 4554 Å, it is possible to follow their separate motions simultaneously by using two cameras with different filters. A photograph of such a barium release (Fig. 6) clearly shows the separated mass motion of neutral and ionized material.

In addition to atomic vapors with their extremely narrow spectral-line emissions, sunlit molecular species have also been studied, usually for temperature measurements. The blue glow of AIO, a diatomic molecule unstable at normal pressures, is observed in the upper atmosphere after the sunlit detonation of high-explosive grenades containing aluminum (12), or the sunlit release of an organometallic vapor, trimethylaluminum (13). The AIO resonance spectrum, as shown in Fig. 7, consists of several bands, each 100 Å wide, in the 5000-Å region, and instrumental resolution of a few angstroms suffices to characterize the temperature responsible for their spectral profiles.

Another release with a quite different objective is currently under investigation by Rosen and Bredohl (14), who are seeking the photochemical origin of NH and NH_2 bands in spectra from comets. In this study, ammonia vapor is released into a sunlit upper atmosphere for observation of the rate of appearance of resonance spectra of NH_2 and NH radicals. The radicals are produced on dissociation of NH_3 following absorption of solar ultraviolet radiation. The first experiments showed that these rates are reasonably fast, and the fuller simulation of cometary spectra may proceed from this study.

Sunlit releases of liquids and solids provide an interesting side effect in some

gaseous releases and explosions (15). Aerodynamic drag on small particles varies enormously over this height region. For example, a high-speed particle with a radius of 0.3 micron, moving horizontally at a height of 80 km, will lose half its velocity by momentum transfer in only 20 m, but at 120 km will travel 20 km before similarly slowing. Thus if an expelled liquid breaks up into small droplets, or if a smoke is ejected as an explosion product, many particles proceed to distances of kilometers before they are finally stopped. Because of this, the sunlit release or detonation of a mixture which forms both a resonance-radiating gas and a light-scattering smoke or mist develops two quite different zones from very early times. The gas expands spherically, at first supersonically, but comes to rest within about 1 second at a radius of a few hundred meters. Over a somewhat longer time, an outer spherical shell of sunlit smoke particles grows at a velocity of about 1 km/sec to a much larger radius. Downward-moving particles eventually form a relatively stationary lower surface as they are halted in the region of 100 km altitude but upward or horizontally moving particles continue to travel radially for many kilometers.

Night-Glowing Releases

Releases that glow without sunlight, unlike the sunlit group, do not act simply as selective mirrors to reflect or scatter sunlight, but instead emit light as a result of chemiluminescent reactions between released material and some species normally present at high altitude. As stated earlier, at altitudes above 85 km, atomic oxygen is an important and highly reactive constituent, reaching its maximum number density at about 110 km. A much lower concentration of atomic nitrogen has also been postulated. One objective of night-glowing releases is to extend wind and diffusion measurements into the night, and a second objective is to identify reactive species such as oxygen and nitrogen atoms and to measure their variation in concentration with height and time.

The system which has been most thoroughly studied in the laboratory is the nitric oxide (NO) reaction with atomic oxygen, which proceeds through two steps in which the net effect is recombination of two oxygen atoms to form a molecule, release of a photon, and regeneration of the NO molecule as a true catalyst (16). Nitric oxide releases into the upper atmosphere (17)

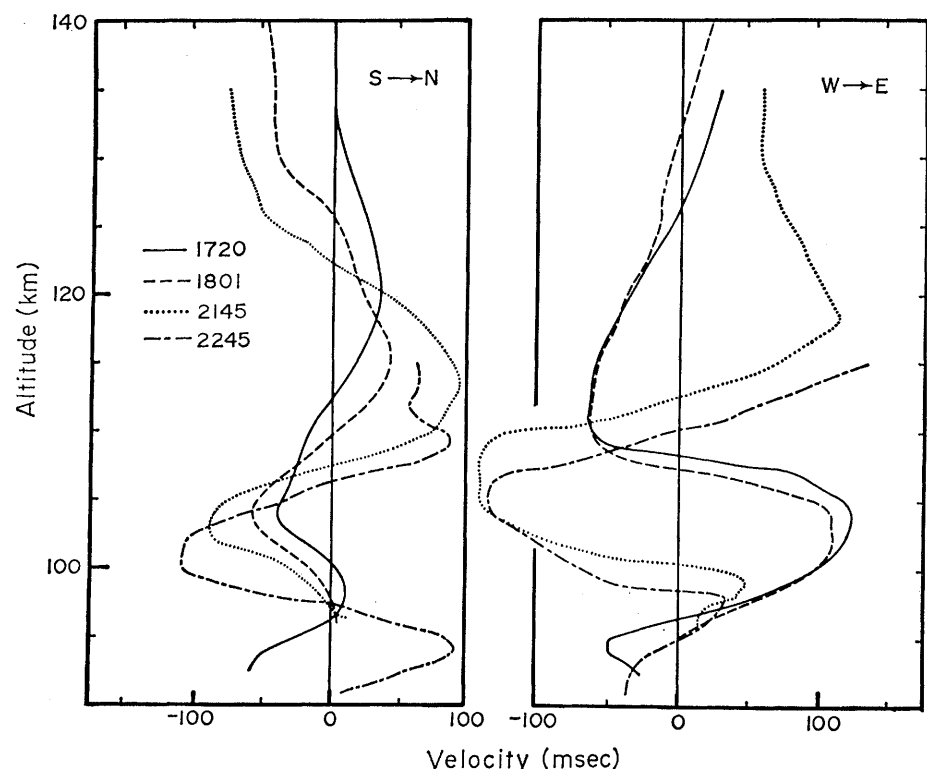


Fig. 5. Typical profiles of NS and EW components of wind velocity as a function of altitude. These four successive profiles, taken over a 5-hour period, show the downward motion of the wind pattern over this period.

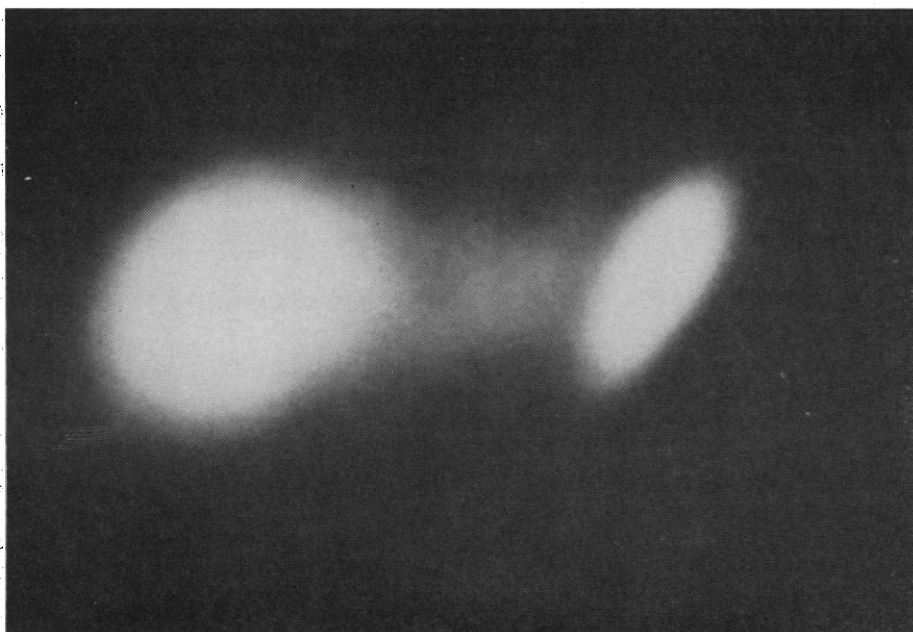


Fig. 6. Release of barium vapor at an altitude of 160 kilometers. Both neutral Ba atoms and ionized Ba^+ were formed in the initial explosive release. Over 500 seconds (between the time of release and the time of this photograph) the ambient wind moved the neutral atoms about 20 kilometers from the release point. The atoms simultaneously diffused spherically to a radius of about 5 kilometers. On the other hand, the released ions were prevented from moving horizontally by the earth's magnetic field lines and were free to diffuse only along these field lines, forming a cylindrical cloud. The source of the dim band of light between the cylinder and the sphere is photoionization of a small fraction of the neutral barium as it moved away from the ionized cloud. [Photograph provided by J. Neuss, Max Planck Institute, Munich]

show an onset of luminescence above 85 km. Relative height-intensity profiles and maximum emission at 110 km are in good agreement with expected atomic oxygen profiles, quite similar in three releases at different times after sunset (8). A still-unexplained feature of the field studies is that the glow intensity of upper-atmosphere releases is over 1000 times as great as would be predicted from extrapolation of laboratory-determined rate constants. Since the expanded trail radius is close to that predicted from aerodynamic theories of jet expansion and is directly related to ambient number density, the NO release may be used in an aerodynamic measurement of density profiles at high altitudes.

The chemiluminescent reactions of two hydrocarbons, ethylene and acetylene, with atomic oxygen have been observed both in the laboratory and in the upper atmosphere. The upper atmosphere release of ethylene (18) gave bright glows, although no well-resolved spectra were obtained. In more recent field experiments, trail releases of acetylene between 90 and 120 km (19) gave bright glows with spectra consisting of C_2 and CH bands in the blue

and yellow, and an OH continuum in the red. This spectrum duplicates those obtained in laboratory studies of acetylene and ethylene with oxygen atoms (20). The absence of any trace of the cyanogen (CN) bands found in laboratory studies of reactions of nitrogen atoms with acetylene suggests a low upper limit to natural atomic nitrogen concentrations.

Certain aluminum-containing releases provide an upper-atmosphere chemiluminescent reaction which is poorly understood but very useful as a tracer. Small (20 g) explosive grenades containing powdered aluminum as one constituent gave persistent (10- to 100-second) glows when detonated at night above 90 km (21), although only an instantaneous flash was observed at lower heights. Grenades containing no aluminum gave no persistent glows at any altitude (22). The emitted light from the glow is a continuum extending throughout the visible spectrum but reaching its peak in the green. Liquid trimethylaluminum has been found to give a similar continuum glow (23). (Despite the highly reactive methyl radicals in trimethylaluminum, no CH or C_2 band emissions are found). The

photon efficiency of trimethylaluminum is high (20 g/km gives a photographable trail for 100 seconds) and it can be easily released at a controlled rate, so it has been adopted for measuring night-time ionospheric winds from 90 km to as high as 180 km.

When trimethylaluminum (or aluminum-containing) grenades are released in sunlight the blue AIO resonance spectrum is found, superimposed on the chemiluminescent (continuum) glow (Fig. 7). This confirms the formation of gaseous AIO as a reaction product, which may then act similarly to NO as a catalyst for recombining oxygen atoms, but at even higher efficiency. About one photon is observed per molecule of trimethylaluminum released, which strongly suggests a catalytic process, since light outputs of non-catalytic chemiluminescent processes rarely exceed one photon per thousand reacting molecules. Another similarity to NO releases is that the onset of the glow occurs only above 85 or 90 km.

An interesting sidelight to the release of trimethylaluminum is that it shows a "reentry" effect. Ejection of the liquid is followed by flash vaporization of about half the contents of each released droplet, while the remainder cools and freezes to provide the heat of vaporization. Frozen drops formed during release above about 115 km continue unimpeded by aerodynamic drag along the same ballistic trajectory as the rocket. Therefore, as the rocket reaches apogee and then returns, it is accompanied by an invisible cloud of trimethylaluminum ice, and on returning to heights below 115 km, this cloud of ice, which has expanded to a radius of several kilometers, is slowed to a negligible velocity by the increasing atmospheric density. There it is warmed both by aerodynamic reentry heating and more slowly by heat exchange with the relatively dense air and again releases vapor which glows for many minutes as it is slowly generated in the 90 to 100 km height region, as seen in Fig. 8. The diffuse cloud soon develops an eddy structure even at a distance of several kilometers from the vehicle trajectory which strongly argues that turbulence observed below 105 km is not caused by vehicle passage.

A series of wind measurements from a single site made possible by the trimethylaluminum trails has led to interesting observations of certain persistent features. For example, in sev-

eral profiles made during a single night, a clockwise rotation of the wind vector at any fixed altitude was found to occur with a rotation period of about 12 hours. The wind pattern moved downward with a similar period (Fig. 5); that is, over 6 hours, the peak northerly wind moved downward to the altitude where the peak southerly wind had been. This behavior has been observed twice (24); thus in these two cases the semidiurnal component of the ionospheric wind pattern was clearly significant. Whether it is a "normal" feature will await a further number of such night series. Removal of the semidiurnal features leaves profiles quite consistent with those predicted from gravity wave theory by Hines (10).

Wind shears are highest in the same altitude region (95 to 115 km), where sporadic E layers, thin sheets of anomalously high ionization, are found. While the correlation is not perfect, it is clear that one of the factors in producing sporadic E is the presence of

such high wind shears. A recent symposium (25) on this topic brought out many problems as yet unexplained, and an extensive series of simultaneous measurements is planned.

Effects on Electron Density

The natural electron density in the daytime ionospheric "E layer" at 100 km altitude is about 10^5 electrons per cubic centimeter, decaying at night to below 10^4 . The daytime layer is responsible for over-horizon radio propagation at frequencies below about 10 megacycles per second. It is formed through photoionization of atmospheric oxygen and nitrogen by solar radiation in the far ultraviolet (below 1026 Å). The total mass of ionized gas is only a few milligrams per cubic kilometer, and it is therefore feasible to increase this electron density locally by the release of an easily ionized chemical. Atomic cesium vapor has an

ionization potential of 3.9 volts, lower than that of any other gas, and can be photoionized by solar radiation at wavelengths as high as 3200 Å. Its photoionization rate in sunlight is about 3×10^{-4} /sec (that is, 1 percent of an injected sample will be ionized in 30 seconds). The ionization rate of molecular oxygen is much lower (less than 10^{-7} /sec), since oxygen, unlike cesium, is not ionized by the abundant solar radiation between 1026 and 3200 Å. (The other major atmospheric constituents have even lower ionization rates than molecular oxygen). Because of this, replacement of only one oxygen molecule in 3000 by cesium would double the electron-production rate in a sunlit "seeded" volume. Of course, losses of electrons by recombination and attachment must be considered in estimating the electron content and lifetime of such an "artificial electron cloud" (26).

In a series of tests along these lines, 2 kg of cesium vapor were injected into

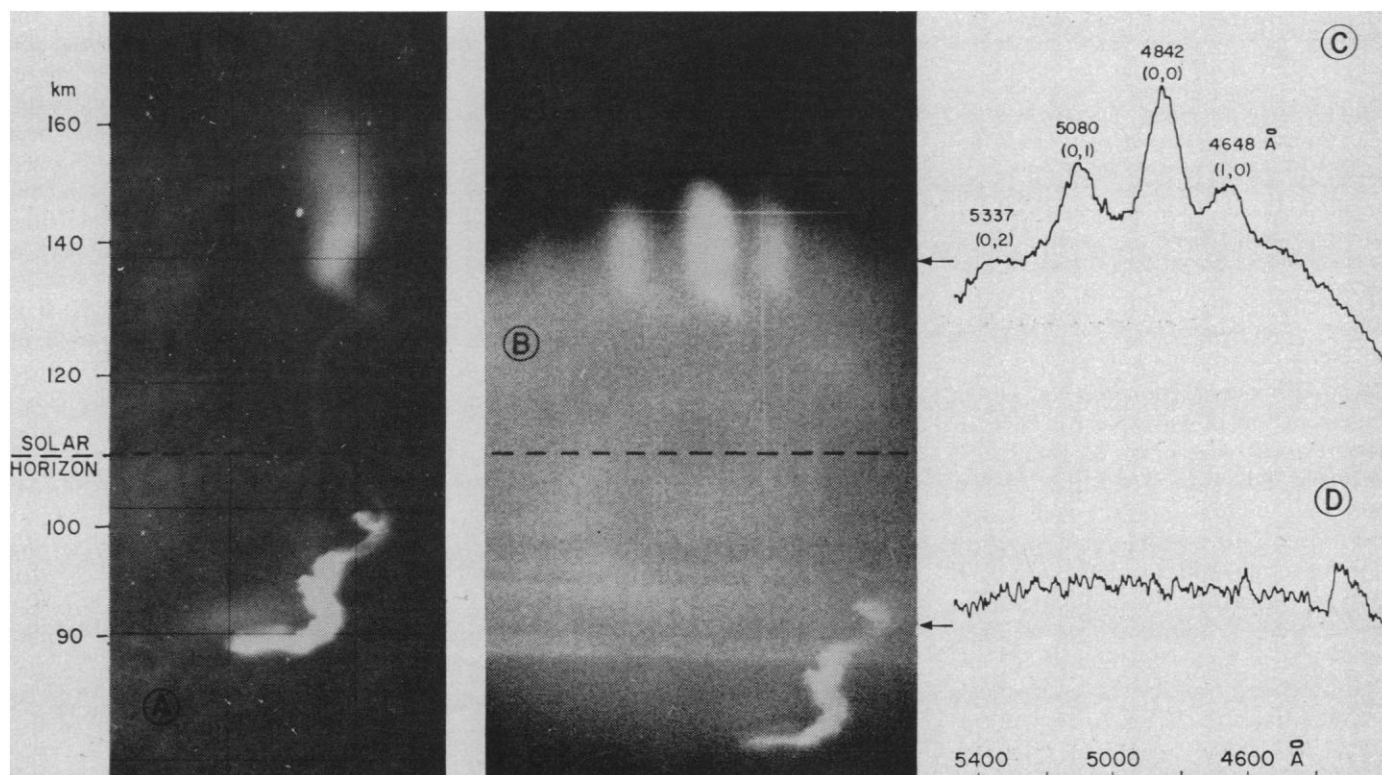


Fig. 7. Chemical trail at twilight. This trail was made by the release of 2 kilograms of trimethylaluminum between 170 and 70 kilometers along the downleg of a rocket trajectory. Both photographs *A* and *B* were made about 100 seconds after the release was completed, and at a time when the trail was sunlit only above 110 kilometers. Photo *A* was taken with an ordinary camera, but photo *B* was taken with a camera equipped with a transmission grating to spread the image into its spectral components (provided by C. D. Cooper, University of Georgia). Photo *A* shows a large trail radius at high altitude, a turbulent zone below 102 kilometers, and a cessation of luminosity below 88 kilometers. The enhanced brightness and radius below 100 kilometers are caused by reentry of a cloud of trimethylaluminum ice. Photo *B* shows four spectrally separated images of the upper (sunlit) portion of the trail, where emission is largely in four AIO resonance bands. The nonsunlit lower portion of the trail shows only a continuum (chemiluminous) emission (with the zero-order image artificially overlaid onto the 4400-Å spectral region). Curves *C* and *D* are densitometer traces of upper and lower parts of photo *B*, with a wavelength scale shown below.

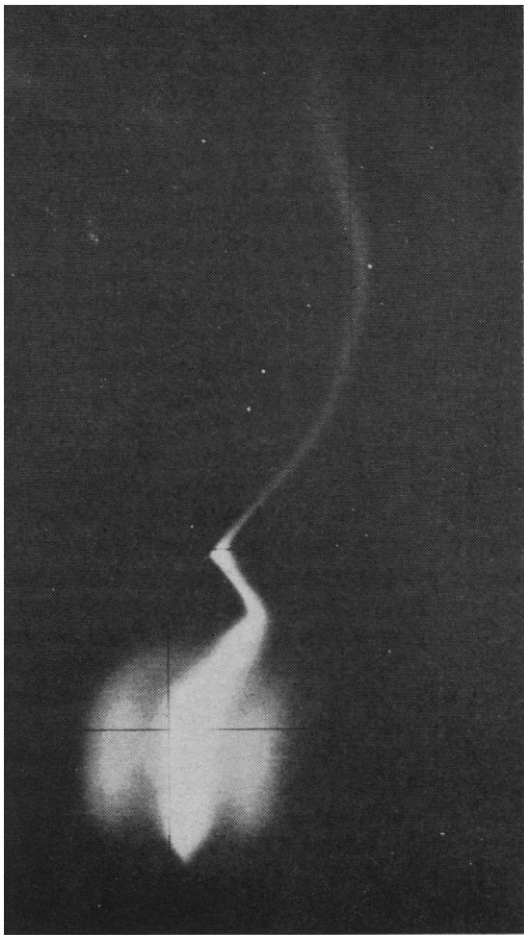


Fig. 8. Photograph of chemiluminous trail showing reentry cloud. This photograph was taken 3 minutes after that of Fig. 3, and shows return of the second rocket to 90 kilometers. Reentry cloud from trimethylaluminum released on upward trajectory forms separate cylinder outside of reentry cloud from release of trimethylaluminum between 150 and 90 kilometers on downward trajectory. Reentry clouds span altitude region from 110 to 90 kilometers.

the atmosphere at altitudes near 100 km by detonation of an explosive mixture. The released gas contained about 10^{26} molecules and atoms, of which 20 percent were cesium atoms. After 1 second, the pressure-equilibrated spherical cloud had an optical radius of about 200 m (measured by photography at the cesium resonance wavelength), equivalent to a cross section of 10^5 m². Transmission of radio-frequency signals between transmitters and receivers separated by 100 to 1000 km, using the cloud as a reflecting relay, showed a prompt onset of propagation when the release occurred. Received signal intensities fluctuated rapidly because of interference among waves reflected from different parts of the cloud, but the average signal intensity at high frequencies was that expected from a reflector with an area of 10^5 to 10^6 m²

and corresponded reasonably well to the observed optical area. The reflected radio signals appeared within a fraction of a second of the detonation, whether the release region was sunlit or dark; thus the ionized region which formed on release did not involve photoionization. The quantitative data suggests that chemical ionization of cesium occurred during the detonation process, with about 0.1 percent of the cesium remaining ionized immediately following expansion.

After release, night clouds decreased in radio cross section, first at higher frequencies, then at lower frequencies, as the electron density decayed. After about 10 minutes, they were usually lost into background noise levels. However, sunlit clouds retained high-frequency reflectivities for much longer times, as photoionization replenished the original electron inventory. These clouds were often lost because they drifted out of the antenna patterns rather than because of decay to background electron density. At altitudes below 95 km, oxidation of cesium vapor, as well as attachment and recombination losses, limited cloud "life," and at heights above 120 km diffusion of neutral cesium vapor rapidly diluted the cloud. Cloud lifetimes were found to be highest at about 100 to 110 km, in a region where no single process dominated the decay of electron density.

Removal of electrons from the normal ionosphere by chemical release has also been demonstrated (27). Even at the region of maximum electron density in the "F region" of the ionosphere between 200 and 300 km, total ionized constituents amount to only a fraction of a gram per cubic kilometer. A 10-kg quantity of an efficient electron-attaching gas, sulfur hexafluoride, was released at midday at a height of about 200 km, just below that of the observed F region maximum electron density. Detection of a target at radio frequencies near the F region maximum-reflection frequency occurred promptly on release, at the correct distance from the radar. This target is presumably due to the local distortion of the natural radio-reflecting surfaces of equal electron density in the ionosphere. The distortion provides an additional discrete reflecting surface between transmitter and receiver. The target grew closer in range with time as the radial diffusion of the gas depleted a region of 10 to

30 km radius. Radar records also showed returns from targets at several much further apparent ranges (delay times). These have been shown to be caused by the formation of additional long-delay paths for radio waves near the center of the depleted region by distortion of electron density profiles. The restoration of the region to a normal radio reflection condition required about 2000 seconds. This time is much too long for isotropic spherical diffusion but is consistent for diffusion through the ends of a cylinder where the electrons seeking to reenter the depleted region can travel only along the earth's magnetic field lines.

Shock- and Acoustic-Wave Studies

The detonation of a high explosive charge—in effect, the sudden injection of a gas at high pressure and temperature—has been very extensively studied at low altitudes, and more recently both theoretical and experimental studies have been carried to altitudes of interest to this survey. Measurements of atmospheric temperature and wind profiles are now made almost routinely by detonation of a series of small grenades along a rocket trajectory, with observation of time and direction of sound arrival at a ground-based microphone array (28). Comparison of travel times and distances for sound waves between successive grenades leads to acoustic velocity. The acoustic velocity V_a is related to the temperature T by the equation

$$V_a = (\gamma RT/M)^{1/2}$$

where γ is the ratio of specific heats at constant pressure and constant volume, R is the gas constant, and M the average molecular weight of the ambient atmosphere. This measurement has been carried out successfully to a height of about 100 km, above which the sound arriving at the ground is severely weakened by several factors.

The first factor is simply the spherical growth of the sound wave, which results in a decrease of total acoustic energy from detonations at longer distances when received at a ground-based detector of fixed area. The second factor, unique to heights above about 80 km, is the attenuation of sound intensity from I_0 to I over a path length L_p according to the equation

$$I/I_0 = \exp - (4L_m L_p / L_s^2)$$

As the mean free path L_m approaches the wavelength of the sound wave L_s , this attenuation acts as a cut-off filter for high-frequency components. For example, an acoustic wave containing a wide spectrum of frequencies will lose 90 percent of its intensity at 30 cycles per second ($L_s = 10$ m) in traveling downward 10 km from a height of 85 km, but in only 0.1 km of travel from a height of 105 km. Even as low a frequency as 0.3 cycle per second ($L_s = 1000$ m) will have similar cut-offs at a height of about 150 km. Acoustic detection of the very low frequencies which reach the earth's surface is difficult because of competing wind noise.

The third source of energy loss from a high-altitude detonation lies in the failure of the released gas to couple its energy into the low-density ambient under certain conditions, which have been analyzed by Groves (29). Since Groves's treatment also provides a clearer understanding of the aerodynamics of chemical releases, a qualitative review of that analysis is worthwhile here. The expansion is shown schematically in Fig. 9. At the instant of injection the released gas has a pressure many million times as high as that of the surrounding air. It expands radially, sweeping up surrounding air into a thin spherical shell, which forms a shock wave. As the expansion continues, the number density within the shock increases until it reaches the maximum value permitted by the aerodynamic properties of air. This value is about 9 times ambient density. At the same time the shock reaches a maximum pressure about 400 times ambient pressure. Radial expansion continues with no further change in shock density or pressure until the pressure of the expanding release gas falls to that in the shock. From this point on, pressures, densities and velocities decay both in the shock wave and in the released gas.

Energy losses from the released gas are high; typically 85 percent of the energy of the release (exact values are dependent on its specific heat ratio γ) is lost into shock-wave formation and expansion to ambient pressure. This energy is obtained from the cooling of the released gas during its expansion. A detailed aerodynamic evaluation shows that a gas sample with initial energy E_0 and temperature T_0 on release at an ambient pressure p_a reaches a final

bubble radius r_1 and temperature T_1 given by

$$r_1 = k(E_0/p_a)^{1/3}$$

and

$$T_1/T_0 = 4\pi k^2/3(\gamma_0 - 1)$$

where k is a nearly constant parameter $= 0.2 \pm .02$ over the entire altitude region of interest, and γ_0 is an average specific heat ratio defined by $\gamma_0 - 1 = nRT_0/E_0$. A typical high explosive with a $\gamma_0 = 1.2$ leads to $T_1/T_0 = 17$ percent, so a detonation providing an initial temperature of 3600°K results in an expanded gas bubble temperature of only 600°K.

The shock wave degenerates into an acoustic sound wave as its velocity decreases toward Mach 1. Inside this wave lies air through which the shock has already passed, and inside this air layer is the spherical bubble of released gas. (In an earlier section, bubble radii following gas release were calculated on the assumption that the final temperature of the released gas was equal to the ambient temperature. It can now be seen that such values are valid if the injected material is released at a temperature about six times ambient temperature. For example, if the injected gas is initially at 1800°K, its final temperature of about 300°K will

equal ambient temperature at 100 km.)

As we take a release (of fixed total energy) to higher altitudes, it sweeps up less and less ambient gas before its own pressure falls to the maximum shock pressure p_m . We eventually reach a height where the released gas no longer sweeps up enough ambient gas to bring the shock pressure in this ambient up to p_m before its own pressure is below p_m . Above this height the maximum shock pressure actually developed is lessened, and eventually we reach a height where the swept-up gas never exceeds ambient pressure and no shock wave develops. For a high explosive weight of 300 g (or for a few kilograms of a gas initially at 300°K) the shock weakens above 110 km and is nonexistent above 145 km. For 300 kg of high explosive, these heights are respectively 140 km and 280 km.

For all these reasons, explosions above 90 km give very weak acoustic signals at the ground. However, in the altitude region between 90 and 130 km, detection of the shock wave near the explosion itself is possible if a grenade is detonated along a chemiluminous trail being simultaneously generated from the same carrier rocket (30). The local compression in the spherical shock wave creates a bright zone at its intersection with the chemiluminous trail,

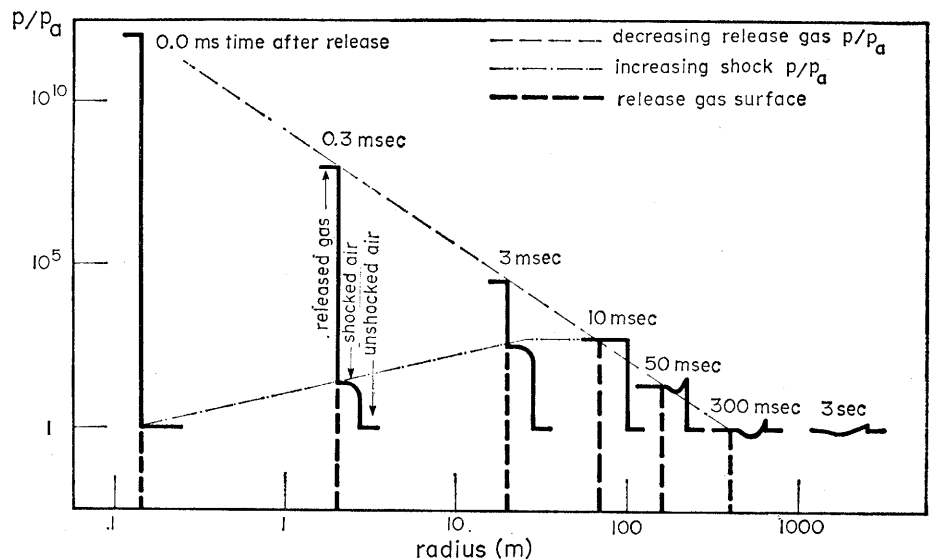


Fig. 9. Early growth of shock wave in the ambient atmosphere formed at surface of expanding sphere of released gas. The schematic calculated example is for 4 kilograms of high explosive detonated at an altitude of 120 kilometers. Horizontal scale is radius r from point of detonation, vertical scale is ratio of pressure at radius r to ambient pressure. Note buildup of shock wave to maximum permitted p/p_a value of 400 at a radius of 30 meters in 5 milliseconds, and shock-wave pressure decay after 10 milliseconds when released gas falls to p/p_a below 400. The released gas completes its expansion at a radius of 400 meters in a time of 0.3 second, while shock wave continues forward at a Mach number decreasing toward unity.

shown in Fig. 10. This zone can be followed photographically in both night-time and twilight releases as it travels along the trail until the shock wave expands to a radius (typically 1 to 2 km) where its pressure decreases to about 20 percent above ambient, and the bright zone can no longer be distinguished. Scaling of the photographic

records of early radius-time history provides a reasonably accurate (± 10 percent) estimate of the decreasing shock velocity, from which the ambient atmospheric temperature can be determined to about ± 20 percent. Several grenades detonated along a single trail can thus be used to provide a temperature profile.

Future Trends

Some types of chemical-release experiments have reached the point where they are reasonably accepted tests of upper atmosphere properties rather than tests of techniques. There are three major directions which further studies using these proven techniques are taking. One direction is toward more closely spaced exploration of time and space patterns, for example, of winds. In the study of wind patterns a simple and inexpensive payload design and measurement technique is essential in order to provide a matrix of several simultaneously measured profiles separated by a few hundred kilometers, repeated at intervals during a single night, to provide meaningful space and time gradients of the flow field. Repetition of this test on several occasions and at several latitudes will be required to determine whether a given pattern is typical and whether seasonal and latitude effects are significant. Extension of measurements into daylight hours by photography from a satellite station against a black sky background appears feasible.

In a second direction, the interrelationships among different properties of the upper atmosphere have increasingly become an important objective of further studies. We have previously mentioned the evaluation of interrelations of neutral and ion motions by the simultaneous observation of mass motions of a barium-atom tracer and a barium-ion tracer. The extension of this same experiment into interplanetary space may permit the mapping of field lines in the region where the magnetic fields of earth and sun meet.

Other experiments in this direction will be accomplished by coordinated launches of several different rocket-borne measuring instruments. One case of interest, mentioned earlier, is the simultaneous measurement of wind shear profiles by chemical releases and of electron density and ion composition profiles by rocket-borne sensors. This study is currently underway to determine whether observed formation of natural ionized layers is related to maxima in the wind shear profiles. A second case of interest is the simultaneous measurement of temperature of profiles in the neutral atmosphere by resonance scatter (at twilight) or by detonations, and of the ion and electron temperatures by rocket-borne charged-particle temperature sensors. The extent to

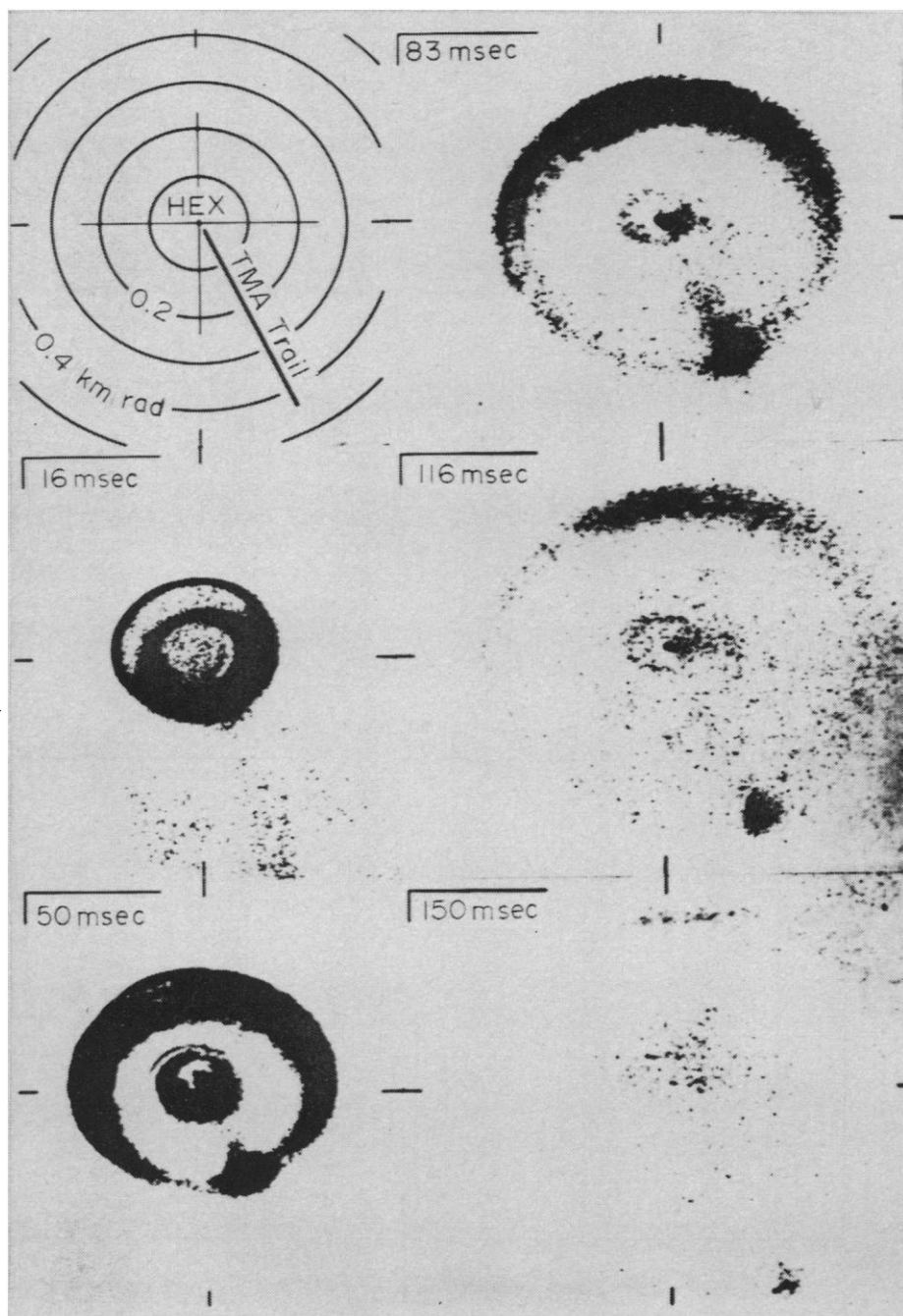


Fig. 10. Early growth of shock wave along trimethylaluminum (TMA) trail, following detonation of 4 kilograms of high explosive at an altitude of 120 kilometers. Sequence of five photographic negatives shows radial growth by movement of bright zone formed at intersection of spherically expanding shock wave and previously released trimethylaluminum trail from same vehicle. (The outward-moving shock is also visible elsewhere because of trimethylaluminum released from its container ruptured by the detonation.) This sequence (provided by W. Manning, USAF ETR) was taken through a telescope connected to a television camera.

which thermal equilibration is a function of altitude among neutral atoms and molecules, ions, and electrons is one of the important areas of ionospheric geophysics in which no direct experimental measurements are as yet available.

A third direction is the "calibration" of less direct but ground-based measurements, which accumulate statistically large quantities of not-always-clear data. For example, movements within ionospheric layers are inferred from ground-based radio-frequency interferometers. Whether these are gross mass motions (winds) or the phase velocities of wave motions is now being investigated by means of simultaneous measurements of wind profiles by chemical release. If the motions are in fact those of winds, their study can reduce the need for the more costly rocket-borne profiles which will always be limited to statistically small samples. As another example, upper-atmosphere motions of electron irregularities are observed (at 200 to 500 km) by the large backscatter radar of the Arecibo Ionospheric Observatory in Puerto Rico. These motions will be compared with direction and velocity of neutral winds up to 250 km determined by chemical releases, to find whether the two motions are similar or generated by a common energy source.

Other chemical releases are still emerging from the stage of testing techniques rather than atmospheric properties and will be incorporated into the

tool kit of the upper-atmosphere scientists as they are brought to the status of proven measurements. Both the techniques of controlled release and of ground-based observations of the releases, spectrally and spatially resolved, need continued improvement. In some areas, this requires increased sophistication in experimental design. Paradoxically, in other areas, simplification of measurement techniques to the most routine level possible is more important, to make feasible the collection of a sufficiently large number of observations for an understanding of the "meteorology" of the ionosphere. What is certain is that imaginative investigators will continue to come forward with novel experimental approaches and interpretations in this fertile field.

References

1. *U.S. Standard Atmosphere, 1962* (Superintendent of Documents, Washington, D.C. 1963).
2. D. R. Bates, *J. Geophys. Res.* **55**, 347 (1950).
3. H. D. Edwards, J. F. Bedinger, E. R. Manring, C. D. Cooper, in *Aurora and Airglow*, E. B. Armstrong and A. Delgarno, Eds. (Pergamon, New York, 1955), p. 122.
4. M. Dubin, NASA Headquarters, Washington, D.C., private communication; C. Henry, thesis, Univ. of Paris (19 June 1964); A. Kochanski, *J. Geophys. Res.* **69**, 3651 (1964); E. Manring, J. Bedinger, H. Knaflich, D. Layzer, *U.S. Nat. Aeronaut. Space Admin. NASA CR-36* (Washington, D.C., 1964); G. V. Groves, *Space Res.* **5**, 1012 (1964).
5. E. R. Manring, J. F. Bedinger, H. Knaflich, *Space Res.* **2**, 1107 (1961); J. E. Blamont and C. de Jager, *J. Geophys. Res.* **61**, 3113 (1962); E. R. Johnson and K. H. Lloyd, *Australian J. Phys.* **16**, 490 (1963); S. P. Zimmerman and K. W. Champion, *J. Geophys. Res.* **68**, 3049 (1963).
6. J. Blamont, M. L. Lory, G. Courtes, *Ann. Geophys.* **17**, 116 (1961).
7. I. S. Shklovskii *Iskusstv. Sputniki Zemli Akad. Nauk SSSR* **4**, 195 (1960).
8. D. Golomb, N. W. Rosenberg, et al., *J. Geophys. Res.* **70**, 1155 (1965).
9. M. Dubin and J. F. Bedinger, *International Quiet Sun Year Instruction Manual 9, Sounding Rocket Research Techniques* (IQSY Secretariat, London, 1964), p. 42.
10. C. O. Hines, *Can. J. Phys.* **38**, 1441 (1960); *Quart. J. Roy. Meteor. Soc.* **89**, No. 379 (1963); *J. Geophys. Res.* **70**, 177 (1965).
11. H. Föppl et al., *Planetary Space Sci.* **13**, 95 (1965).
12. B. Authier, J. Blamont, G. Carpentier, M. Hersé, *Compt. Rend.* **256**, 3280 (1963).
13. N. W. Rosenberg, D. Golomb, E. F. Allen, *J. Geophys. Res.* **69**, 1451 (1964).
14. B. Rosen, *Rev. Franc. Astronaut.* **1965**, 18 (1965); H. Bredohl, I. Dubois, L. Gausset, *Bull. Soc. Roy. Sci. Liege* **12**, 820 (1964).
15. N. W. Rosenberg, *J. Geophys. Res.* **68**, 3057 (1963).
16. H. P. Broida, H. I. Schiff, T. M. Sugden, *Trans. Faraday Soc.* **458**, 259 (1961).
17. J. Pressman, L. M. Aschenbrand, F. F. Marmo, et al., *J. Chem. Phys.* **25**, 187 (1956).
18. M. Zelikoff, F. F. Marmo, et al., *J. Geophys. Res.* **63**, 31 (1958).
19. C. D. Cooper, in *U.S. Air Force Cambridge Res. Lab. Environ. Res. Paper No. 15, Project Firefly 1962* (1964), p. 122 (available from CFSTI, Springfield, Va. 22151).
20. N. Jonathan and P. Doherty, *ibid.*, p. 393.
21. E. R. Johnson and K. H. Lloyd, *Australian J. Phys.* **16**, 490 (1963).
22. N. W. Rosenberg, D. Golomb, E. F. Allen, *J. Geophys. Res.* **68**, 3328 (1963).
23. ———, *ibid.*, p. 5895.
24. N. W. Rosenberg and H. D. Edwards, **69**, 2819 (1964).
25. "Symposium Sporadic E," *Radio Science* (Feb. 1966).
26. F. F. Marmo, L. M. Aschenbrand, J. Pressman, *J. Am. Rocket Soc.* **30**, 523 (1963); P. B. Gallagher and R. A. Barnes, *J. Geophys. Res.* **68**, 2987 (1963); J. W. Wright, *ibid.*, p. 3011; N. W. Rosenberg and D. Golomb, *Progr. Astronaut. Aeronaut.* **12**, 395 (1963).
27. D. Golomb, N. W. Rosenberg, J. W. Wright, R. A. Barnes, *Space Res.* **4**, 389 (1963); M. A. MacLeod and D. Golomb, *U.S. Air Force Cambridge Res. Lab. Environ. Res. Paper No. 101 AFCRL-65-287* (available from CFSTI, Springfield, Va. 22151).
28. W. Nordberg, *Aeronaut. Astronaut.* **2**, 48 (1964); in *International Quiet Sun Year Instruction Manual 9, Sounding Rocket Research Techniques* (IQSY Secretariat, London, 1964).
29. G. V. Groves, *J. Geophys. Res.* **68**, 3033 (1963).
30. N. W. Rosenberg, *ibid.* **69**, 2323 (1964).

Plant Pathology and Human Welfare

A. J. Riker

Diseased plants have always been with us and influenced our well-being. The history of mankind through the ages has been the story of hungry men in search of food. Tribes that tended sheep or cattle for their own

food needed forage for their animals as well. The desire for food and forage has brought on many conflicts, small and large, from the beginning of time.

Diseases of plants have causes similar to those among animals and man. In

early times, physicians using medical terms wrote about plant diseases—even though plants do not feel ease or disease as men do. But plants with disease may be so impaired that their usefulness to themselves or to mankind is seriously reduced. With the dawn of history we find reports of famine resulting from mildew and rust, induced by fungi. Certainly, plant diseases were troublesome even in the earliest historic times. Doubtless they were present in evolutionary times, as fossils show. Many of the extinct plants probably had diseases that hastened their disappearance.

How plant diseases developed is not definitely known. Probably when weakened plants died, various microorga-

The author is professor emeritus of plant pathology at the University of Wisconsin, Madison 53706.